Septotemporal variation in dynamics of theta: speed and habituation

James R. Hinman, Stephanie C. Penley, Lauren L. Long, Monty A. Escabí and James J. Chrobak

J Neurophysiol 105:2675-2686, 2011. First published 16 March 2011; doi:10.1152/jn.00837.2010

J Neurophysiol 105: 2675–2686, 2011.
First published March 16, 2011; doi:10.1152/jn.00837.2010.

Septotemporal variation in dynamics of theta: speed and habituation

James R. Hinman,[1] Stephanie C. Penley,[1] Lauren L. Long,[1] Monty A. Escabí,[1,2,3] and James J. Chrobak[1]

Departments of [1]Psychology, [2]Biomedical Engineering, and [3]Electrical and Computer Engineering, University of Connecticut, Storrs, Connecticut

Submitted 1 October 2010; accepted in final form 15 March 2011

Hinman JR, Penley SC, Long LL, Escabí MA, Chrobak JJ. Septotemporal variation in dynamics of theta: speed and habituation. *J Neurophysiol* 105: 2675–2686, 2011. First published March 16, 2011; doi:10.1152/jn.00837.2010.—Theta (6–12 Hz) field potentials and the synchronization (coherence) of these potentials present neural network indices of hippocampal physiology. Theta signals within the hippocampal formation may reflect alterations in sensorimotor integration, the flow of sensory input, and/or distinct cognitive operations. While the power and coherence of theta signals vary across lamina within the septal hippocampus, limited information is available about variation in these indices across the septotemporal (long) or areal axis. The present study examined the relationship of locomotor speed to theta indices at CA1 and dentate gyrus (DG) sites across the septotemporal axis as well as in the entorhinal cortex. Our findings demonstrate the dominant relationship of speed to theta indices at septal sites. This relationship diminished systematically with distance from the septal pole of the hippocampus at both CA1 and DG sites. While theta power at entorhinal sites varied in relation to speed, there were no differences across the areal axis of the entorhinal cortex. Locomotor speed was also related to changes in theta coherence along the septotemporal axis as well as between the hippocampus and entorhinal cortex. In addition to the speed-related variation, we observed a decrease in theta power at more temporal hippocampal sites over repeated behavioral testing within a single day that was not observed at septal sites. The results outline a dynamic and distributed pattern of network activity across the septotemporal axis of the hippocampus in relation to locomotor speed and recent past experience.

theta rhythm; hippocampus; entorhinal cortex; synchrony; electroencephalogram; rat

THE LAMINAR ORGANIZATION of the hippocampus (HPC) provides an ideal anatomy for the generation of large-amplitude local field potentials (LFPs). Theta (6–12 Hz) LFP oscillations are generated by the summation of synchronous excitatory and inhibitory potentials as well as intrinsic membrane potentials (e.g., Bragin et al. 1995; Brankack et al. 1993; Buzsaki 2002; Green and Arduini 1954; Leung 1985; Petsche et al. 1962). In general, the theta signal reflects moment-by-moment variation in the synchronization of afferent input impinging upon the somatodendritic field of hippocampal neurons. Studies have linked changes in theta LFPs to cognitive variables in several mammals (see, e.g., Montgomery et al. 2009; Rizzuto et al. 2006; Ulanovsky and Moss 2007; see Jutras and Buffalo 2010 or Nyhus and Curran 2010 for reviews), while variation in the theta signal in the rodent has often been linked to locomotor speed and sensorimotor integration (see Bland and Oddie 2001; Sinnamon 2006; Wyble et al. 2004 for reviews).

Early reports on the behavioral correlates of theta noted its prominence during locomotion and relation to running speed (Feder and Ranck 1973; McFarland et al. 1975; Teitelbaum and McFarland 1971; Vanderwolf 1969; Whishaw and Vanderwolf 1973). The increase in theta power in relation to speed has been confirmed in studies examining the septal pole of the HPC (Bouwman et al. 2005; Rivas et al. 1996), although Maurer and colleagues (2005) suggested variability in the role of speed at more temporal aspects of the HPC.

There is considerable topographic organization in the afferent input to the HPC. Inputs from the entorhinal cortex (EC) define three domains along the septotemporal (long) axis based upon the band of origin in the EC (Dolorfo and Amaral 1998a, 1998b; Witter 2007). Prominent amygdala inputs preferentially target more temporal levels of the HPC (see Pitkanen et al. 2000 for review), while several subcortical neuromodulatory inputs exhibit variation across the septotemporal axis (Amaral and Kurz 1985; Gage and Thompson 1980; see also Thompson et al. 2008 for review).

The present study examined the relationship between speed and various measures of theta across the septotemporal axis of both CA1 and dentate gyrus (DG), as well as in medial (MEA) and lateral (LEA) entorhinal areas. We demonstrate that locomotor speed is a prominent predictor of theta power and coherence in the septalmost aspect of the HPC and that there is a decrease in the relationship between speed and theta with distance from the septal pole. Furthermore, we observed decreases in theta power over repeated behavioral testing within a single day at more temporally located electrode sites without any decrement at septal sites. This habituation-related decrease was unrelated to locomotor speed. The latter suggests that theta power can be sensitive to the recent past experience of the animal. The results are discussed with regard to anatomy, septotemporal differentiation within the HPC, as well as the utility of theta measures as indices of neural network function.

MATERIALS AND METHODS

Animals and surgical procedures. Six adult male Fischer 344 rats were used in this study. The animals were individually housed in a temperature-controlled room and maintained on a 12:12-h light-dark cycle. All procedures were performed according to protocols reviewed and approved by the University of Connecticut's Institutional Animal Care and Use Committee and were in accordance with the guidelines set forth by the National Institutes of Health.

Rats were anesthetized with a ketamine cocktail (4 ml/kg consisting of 25 mg/ml ketamine, 1.3 mg/ml xylazine, and 0.25 mg/ml acepromazine). After a midline scalp incision, burr holes were drilled in the skull over the HPC and three electrode arrays were positioned

Address for reprint requests and other correspondence: J. J. Chrobak, Dept. of Psychology, Univ. of Connecticut, 406 Babbidge Rd., U-1020, Storrs, CT 06269-1020 (e-mail: james.chrobak@uconn.edu).

along the septotemporal extent of the HPC, while a fourth array was positioned in the EC. The following coordinates were used for each of the four arrays: septal HPC (AP −3.0, ML 2.5, DV 3.0); intermediate HPC (AP −5.0, ML 5.0, DV 5.0); temporal HPC (AP −6.5, ML 5.5, DV 7.0); EC (AP −6.0 to −8.0, ML 6.5, DV 6.5–7.5). Each electrode array consisted of four linearly spaced 50-μm tungsten wires (16 total electrodes; California Fine Wire, Grover Beach, CA), arranged and spaced with fused silica tubing (Polymicro Tubing, Phoenix, AZ). All electrodes were attached to female pins (Omnetics, Minneapolis, MN) secured in a rectangular five by four pin array. Two stainless steel watch screws driven into the skull above the cerebellum served as indifferent and ground electrodes. Two or more additional support screws were positioned over the anterior aspect of the skull, and the entire ensemble was secured with dental acrylic. Rats were allowed to recover for 1 wk after surgery.

Behavioral performance and electrophysiological data acquisition. Rats were food deprived to 85% of their ad libitum weight and trained to run on a linear track (10 × 140 cm) for chocolate sprinkles. Recording sessions consisted of five individual recording sessions separated in time within a single day (Fig. 1*A*). The end of the first recording session marked *time 0* (T_0 or baseline). The subsequent four sessions were initiated at T_5, T_{20}, T_{60}, and T_{120} (minutes). Each of the five sessions required the rat to complete a minimum of 50 trials, where a single behavioral trial consisted of the rat running from one end of the track to the other end. After the rat completed 50 trials, it was returned to its home cage on a table adjacent to the linear track until it was time to start the next recording session. No changes were made to the track or the room between recordings.

Wide-band electrical activity was recorded (1–1,894 Hz, 3,787 samples/s) during each recording session with a Neuralynx data acquisition system (Bozeman, MT). Light-emitting diodes attached to the headstage were tracked via a camera (33 samples/s) positioned over the linear track, thus allowing for an off-line record of the animals position over time. To calculate locomotor speed, the positional difference between successive tracking samples was calculated and then low-pass filtered (cutoff = 0.25 Hz) in order to minimize the contribution of head movements and movement artifacts to the overall speed of the rat. A representative filtered position vs. time trace is shown in Fig. 1*B*. Such traces were used to calculate instantaneous and mean speed during designated intervals.

All data analysis was conducted with custom-written programs in MatLab (The MathWorks, Natick, MA) or in SPSS (SPSS, Chicago, IL). Movement-related data were visualized as a state-space plot (position vs. velocity; see Fig. 1*C*). To exclude data recorded during consumption of sprinkles and turning behavior, a physical threshold 14 cm from each end of the maze was set (Fig. 1, *B* and *C*) and any trial during which the rat's speed decreased below 5 cm/s was discarded. The resulting data set contained an average of 46.4 ± 0.88 (SE) trials per recording.

Spectral indices. Power spectral density estimates were obtained by Welch's averaged modified periodogram method (Welch 1967). For each trial run, the average power in the 6- to 12-Hz band and the corresponding mean speed for each nonoverlapping 1.5-s interval were calculated. Theta phase was obtained from the Hilbert transform of the theta band pass-filtered signal (6–12 Hz), and then the instantaneous frequency was determined by calculating the change in phase divided by the change in time between each sample. Average theta frequency was calculated over each 1.5-s trial segment (see also Jeewajee et al. 2008).

To calculate coherence, trials (as defined above) were sorted based on mean speed (slowest to fastest), and the EEG signals were concatenated into a single continuous string of data (Roark and Escabi 1999; see also Sabolek et al. 2009), such that each recording session (at T_0, T_5, etc.) generated a series of 20-s-long data strings with different mean speeds. Thus the slowest trials totaling 20 s were concatenated, the next slowest totaling 20 s were concatenated, and so forth for all trials [number of concatenated data strings per recording = 5.47 ± 0.11 (mean ± SE)]. Coherence values (Bullock et al. 1990) for each channel pair were computed by the Welch periodogram estimation procedure with a spectral resolution of ~2 Hz (see below).

Each spectral index (power and coherence) from each electrode (or electrode pair) was separately subjected to a simple linear regression analysis that included the mean speeds and the spectral index for the corresponding period of time in order to assess the relationship between locomotor speed and each of the spectral indices. Thus each electrode or electrode pair yielded a single correlation coefficient (r value) for each spectral index. r values near 1 indicate that locomotor speed and the corresponding spectral index are linearly associated, such that a net increase in speed leads to a linear increase in the spectral index. Values near zero indicate no relationship between locomotor speed and spectral index.

Electrode recordings within each septotemporal quartile of the DG and CA1 (e.g., septal 25%; Fig. 1*F*) as well as those in the MEA and LEA were grouped separately to determine whether that region had a mean r value different from zero with a t-test. A nonzero mean for a region's speed r value distribution indicates that that spectral index is significantly speed modulated either positively or negatively (Lorch and Myers 1990). Additionally, a simple linear regression analysis was conducted on the speed r values for DG and CA1 along with the distance from the septal pole (in mm) as an explanatory variable, thus demonstrating whether the speed modulation of each spectral index varied along the septotemporal axis.

Statistics: coherence analysis. A significance estimation procedure was devised in which the coherence estimate was compared with that of signals with identical magnitude spectrum but with zero phase coherence. For each channel pair, the cumulative distribution of the frequency-dependent coherence values was created by randomizing the phase spectrum of the signals while preserving the magnitude spectrum, calculating the coherence for the phase-randomized signals, and bootstrapping the procedure 250 times (Efron and Tibshirani 1993). This procedure guarantees that the signal magnitude spectrums are identical but have no linear association, because the phase or time information has been removed. The coherence distribution obtained via bootstrapping the procedure was used to determine a significance threshold for each frequency band (2-Hz resolution), below which 95% of the shifted null hypothesis coherence values fell (i.e., the null hypothesis; see also Sabolek et al. 2009).

Only regions of the nonshuffled signal coherences falling above the 95% threshold were considered significant. For each channel pair, the statistically significant area in the theta (6–12 Hz) range was calculated and normalized by the frequency ranges (expressed as average coherence value per Hz) to facilitate comparison of different frequency ranges. Finally, the coherence value was normalized for bandwidth and a new zero point, with the resulting normalized coherence values falling between 0 and 1.

Statistics: habituation analysis. To assess any changes in theta power over the repeated recording sessions, a linear regression analysis was conducted that included the mean speeds and four orthogonal dummy-coded categorical variables for the five recording time points (e.g., T_0, T_5, etc.) as explanatory variables. Each electrode site yielded a single standardized regression coefficient [β value, where $\beta = b(SD_x/SD_y)$] for each of the explanatory variables. The resulting β-values indicate how theta power changes in relation to the baseline recording while controlling for speed. Thus a significant nonzero mean β-value distribution indicates that theta power increased/decreased significantly from baseline. The resulting distributions of β-values were assessed by septotemporal position (distance from the septal pole; see Fig. 5*B*) and grouped by septotemporal quartiles (see Fig. 1*F*; see also Sabolek et al. 2009) for both CA1 and DG sites, or for MEA or LEA sites for EC electrodes. Repeated-measures ANOVA and individual t-tests were used to compare the distribution of β-values at T_5, T_{20}, T_{60}, and T_{120} for each anatomic region.

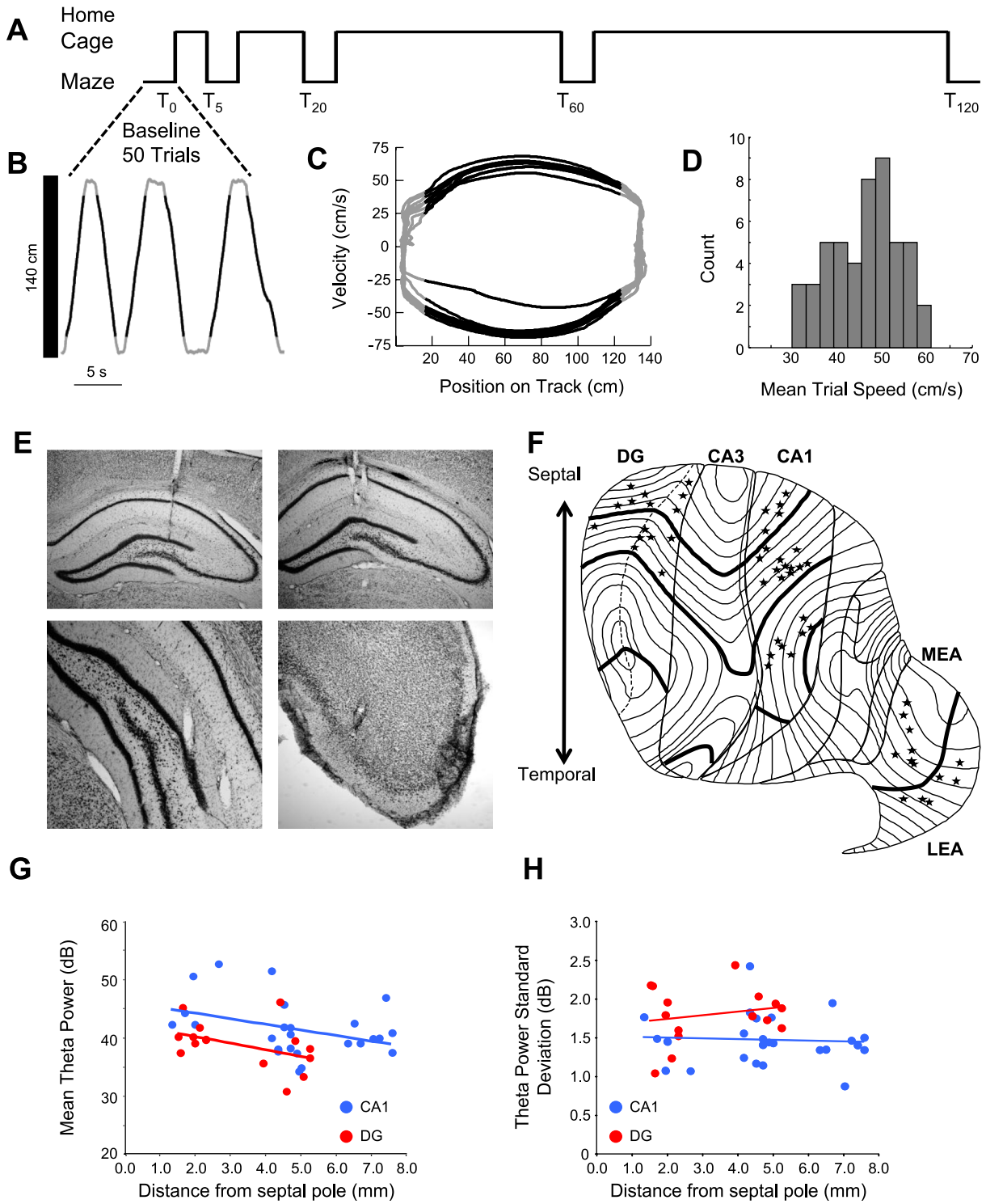

Fig. 1. Experimental timeline and electrode locations. *A*: a series of 5 recordings within a single day were obtained from each rat. The end of the baseline recording marked *time zero* (T_0) and then recordings were initiated at T_5, T_{20}, T_{60}, and T_{120} (minutes). Each recording required the rat to complete 50 traversals of the linear track. Between recordings rats sat in their home cage on a table adjacent to the linear track. No changes were made to the experimental environment between recordings. *B*: the position of a rat along the 140-cm linear track over time during 6 consecutive trials is shown. Black lines overlaid on the gray trace indicate the portion of each track traversal that was considered as an individual trial. *C*: the rat's velocity as a function of position on the track is shown for the 6 trials shown in *A* + the following 6 consecutive trials. Velocity is depicted instead of speed in order to illustrate the similarity in running behavior in both directions. Again the black lines indicate the portion of each traversal that was included as a single trial in further analyses. *D*: distribution of mean trial speeds for an entire single recording session. *E*: photomicrographs of representative recording sites in septal dentate gyrus (DG; *top left*), septal CA1 (*top right*), midseptotemporal DG (*bottom left*), and entorhinal cortex (EC; *bottom right*). *F*: flatmap representation of the hippocampal formation with all recording locations indicated by stars. The septal pole of the hippocampus is located at *top* and the temporal pole at *bottom*. The thick lines mark the boundaries between the hippocampal quartiles, as well as the boundary between medial (MEA) and lateral (LEA) entorhinal areas. *G*: baseline theta power values as a function of distance from the septal pole. Theta power tended to be slightly lower in both CA1 and DG with greater distance from the septal pole. *H*: despite the lower theta power values with greater distance from the septal pole, the standard deviation of theta power values at a given site did not vary as a function of distance from the septal pole.

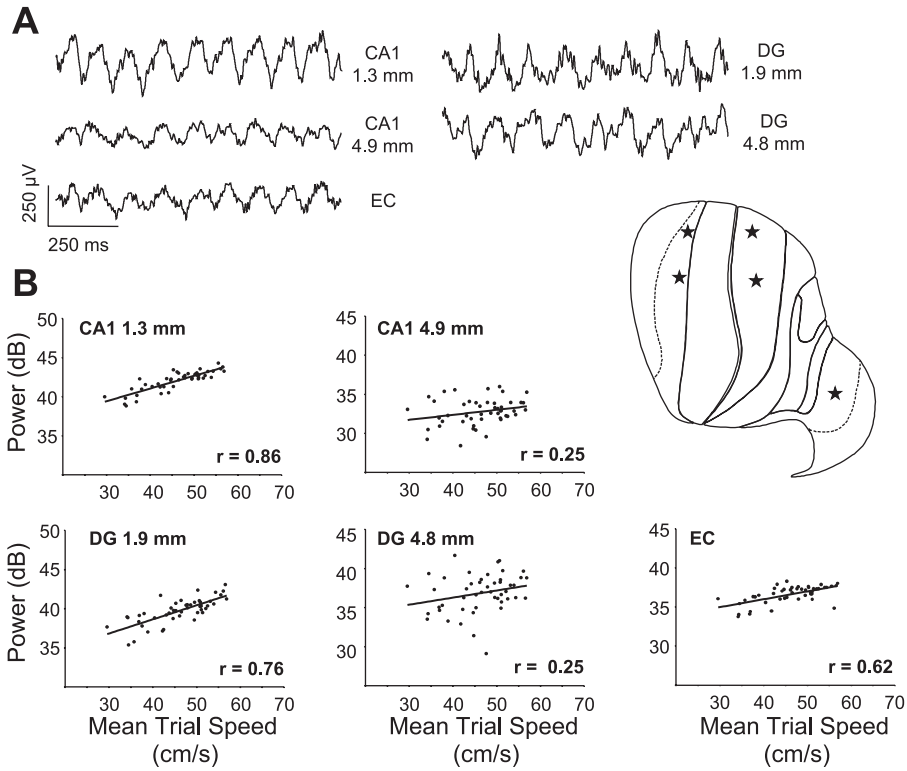

Fig. 2. Variable speed modulation of theta power. *A*: local field potential traces simultaneously recorded from 2 septotemporal levels of CA1 and DG as well as 1 site in EC from a single rat. Note the prominent theta oscillations present at all recording locations. The distance from the septal pole is indicated for the CA1 and DG recording sites. *B*: each scatterplot shows the relationship between mean trial speed and theta power for the 5 simultaneously recorded sites shown in *A* during the baseline recording only (~50 trials). The distances of the CA1 and DG recording sites from the septal pole are displayed at the *top* of each plot, and the correlation coefficient (*r*) is displayed at the *bottom* of each plot. Note the strong relationship between speed and theta power at the septal CA1 and DG sites, as well as the EC site, but that relationship decreases at the more temporal sites. *Right*: flatmap representation of the hippocampal formation with stars indicating the 5 recording locations.

Histology. After the completion of recordings, rats were anesthetized with Euthasol (pentobarbital sodium solution) and transcardially perfused with ice-cold saline followed by 4% paraformaldehyde in 0.1 M phosphate buffer (pH 7.2). Brains were sliced (50-μm sections) with a vibratome (Vibratome Series 1500), mounted, and Nissl stained with thionin. All electrode positions were verified and categorized according to laminar and septotemporal position. Septotemporal distances between electrode positions were determined by noting the location of each electrode position on a flatmap representation of the HPC (Swanson et al. 1978). Each section of a flatmap represents ~200 μm of tissue, and so fairly accurate approximations of the relative distance between electrodes could be determined by counting the number of sections between two electrodes. Photomicrographs of relevant electrode tracks were captured with a Nikon microscope connected to a Spot RT camera system, digitized, and prepared for presentation with Adobe Photoshop 7.0.

RESULTS

Electrodes were positioned at sites primarily within stratum moleculare or stratum granulosum of the DG ($N = 15$), while CA1 ($N = 25$) sites spanned from the ventral aspect of stratum pyramidale to stratum lacunosum moleculare with the majority of sites within stratum radiatum (Fig. 1*E*). In the areal direction, DG placements ranged from 1.6 to 4.8 mm from the septal pole (within the septal and midseptotemporal regions), while placements in CA1 ranged more broadly from 1.3 to 7.6 mm from the septal pole. Electrode placements within the superficial layers of the EC included sites in the medial ($n = 7$) and lateral ($n = 6$) subdivisions that were dispersed across lateral, intermediate, and medial bands (Fig. 1*E* for MEA sites; see also Supplemental Fig. S1 for LEA EC sites).[1]

At all electrode sites, visual inspection and power spectral density confirmed the presence of theta while rats shuttled between ends of a linear track for a food reward (Fig. 1, *B–D*). The power of theta varied according to laminar position, as has been well described in the septal HPC (see Bragin et al. 1995), with sites nearest the hippocampal fissure within stratum moleculare of DG and stratum lacunosum moleculare of CA1 yielding the largest-amplitude signals.

We observed a slight decrease in theta power of roughly 3–5 dB when comparing sites in the septalmost quartile (both DG and CA1) to sites in homotopic positions in the second and third quartiles (Fig. 1*G*, Fig. 2*A*, Table 1). To some extent the difference in theta power may reflect anatomic differences in the density of afferent inputs involved in the generation of LFPs and/or the density of the dendritic fields in which those

[1] Supplemental Material for this article is available online at the Journal website.

Table 1. *Theta power by HPC quartile and within MEA/LEA*

	CA1-Q1	CA1-Q2	CA1-Q3	DG-Q1	DG-Q2	MEA	LEA
Baseline (mean + SE)	46.3 ± 2.2	40.1 ± 1.4	40.7 ± 1.0	40.3 ± 0.8	37.1 ± 1.9	33.5 ± 1.9	32.4 ± 1.1
Baseline (SD + SE)	1.3 ± 0.1	1.6 ± 0.1	1.4 ± 0.1	1.7 ± 0.1	1.9 ± 0.1	2.0 ± 0.1	2.0 ± 0.1
Baseline (range + SE)	6.2 ± 0.9	7.5 ± 0.4	7.2 ± 0.6	7.9 ± 0.7	9.0 ± 0.4	7.5 ± 0.4	7.2 ± 0.6

Baseline values are expressed as dB relative to 1 μV. HPC, hippocampus; Q, quartile; DG, dentate gyrus; MEA, medial entorhinal area; LEA, lateral entorhinal area.

afferents terminate. Despite the differences in absolute power, sites across the septotemporal axis of both DG and CA1 exhibited similar amounts of variability in theta power (see Table 1).

Theta power and locomotor speed across the septotemporal axis of the HPC. All electrode sites located in the septalmost HPC exhibited a prominent increase in theta power as a function of running speed. Initial visual inspection of the relationship between speed and theta power for all electrodes within a given animal revealed clear variation in this relationship throughout the hippocampal formation (Fig. 2*B*, Fig. 3, *A* and *D*). Examples from two rats during the baseline recording show the relationship between speed and power from simultaneously recorded electrodes at multiple septotemporal levels of CA1 and DG, as well as in EC (Fig. 2*B*, Fig. 3*A*). As can be seen, the strength of the correlation between speed and theta power varies with distance from the septal pole in CA1 and DG for these examples. Results are also shown from three simultaneously recorded CA1 sites (Fig. 3*A*), where the strength of the relationship varies systematically along the long axis. For additional information on the distribution of regression coefficients (*b* values, slopes) at CA1 and DG sites across the long axis as well as EC see Supplemental Fig. S2.

Thus speed accounted for a significant portion of the variability in theta power at the septalmost electrode sites, while sites located more temporally in each individual animal exhibited a clear decrease in the relationship between speed and theta power. To quantify this change along the septotemporal axis of DG and CA1, we analyzed the data two ways. First, we conducted a regression analysis using the septotemporal position of each electrode (millimeters from septal pole) and the corresponding r value (for speed vs. power) for that electrode. The relationship of speed to theta power significantly decreased along the septotemporal axis of CA1 ($N = 25$, $r = -0.69$, $P < 0.0005$; Fig. 3*B*). While there was a clear trend for a decrease in the relationship of speed to theta power along the septotemporal axis of the DG, this relationship was not significant ($N = 15$, $r = -0.38$, $P = 0.16$; Fig. 3*B*). It should be noted that DG sites did not extend beyond roughly 5 mm from the septal pole and no DG sites were located in the temporal 50% of the HPC (Fig. 1*F*, Fig. 3*B*).

Although the speed modulation of theta power decreased along the septotemporal axis, this does not demonstrate whether sites at more temporal levels exhibited a significant relationship between speed and theta power. To determine whether theta power at different septotemporal levels of DG and CA1 was significantly related to speed, we grouped elec-

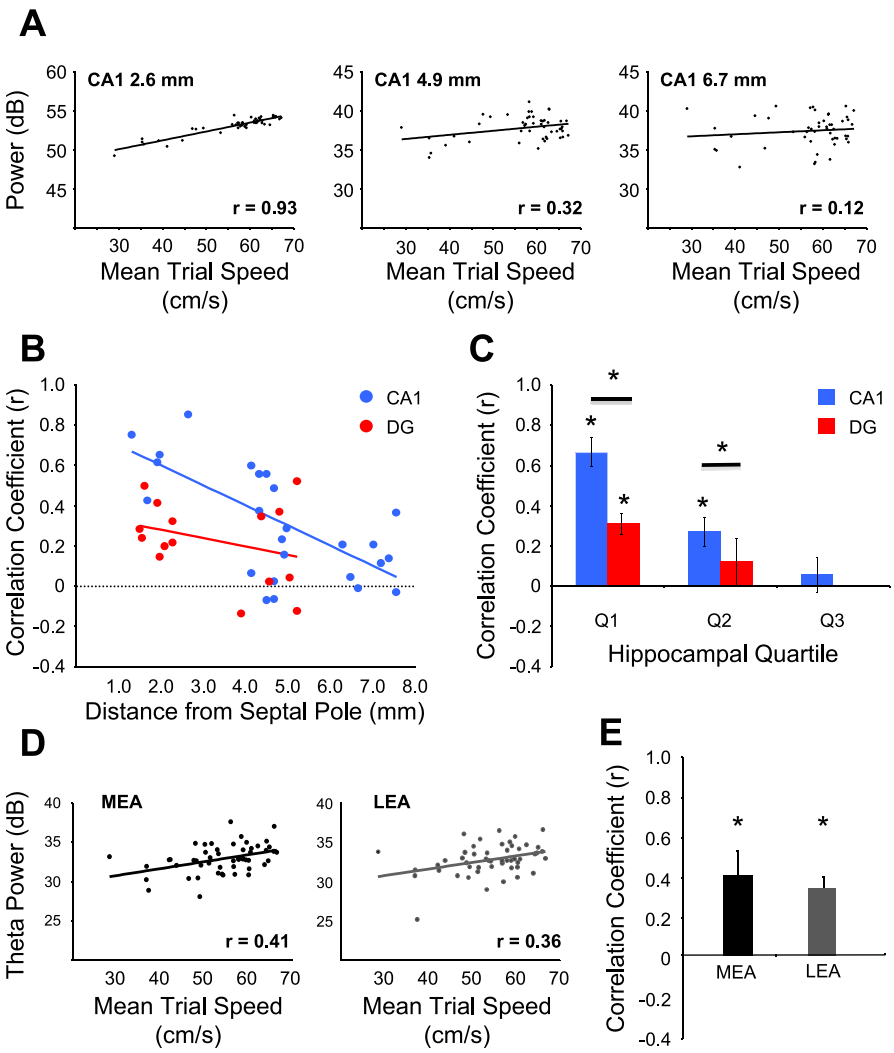

Fig. 3. Variation in speed modulation of theta power throughout the hippocampal formation. *A*: the relationship between mean trial speed and theta power for 3 simultaneously recorded sites along the septotemporal axis of CA1 is shown during the baseline recording only (~50 trials). The distance of each recording site from the septal pole is displayed in each plot along with the correlation coefficient. Note the decrease in the correlation coefficients with increasing distance from the septal pole. *B*: the relationship between distance from the septal pole and the speed vs. theta power correlation coefficients for each CA1 and DG electrode is shown in the scatterplot. A significant decrease in the CA1 correlation coefficients as a function of distance from the septal pole can be seen, while there was a trend for a decrease in DG. *C*: all CA1 and DG electrodes were grouped according to septotemporal quartile in order to assess whether theta power was significantly speed modulated in each region. Theta power was significantly speed modulated in the 1st and 2nd quartiles of CA1 (*$P < 0.01$, t-test), but only in the 1st quartile of DG. Additionally, there was greater speed modulation of theta power in CA1 than in DG (*$P < 0.01$, t-test). *D*: scatterplots, as in *A*, of the relationship between mean trial speed and theta power for 2 simultaneously recorded electrode sites in EC, with 1 site in MEA and the other in LEA, during the baseline recording only (~50 trials). *E*: mean correlation coefficients for MEA and LEA, where theta power was significantly modulated by speed in both areas (*$P < 0.01$, t-test).

trodes for each HPC quartile and conducted *t*-tests on the distribution of correlation coefficients (*r* values). A significant relationship between theta power and speed was observed for electrode sites within the first two quartiles of CA1 [1st: $t(4) = 9.25$, $P < 0.001$; 2nd: $t(11) = 3.79$, $P < 0.005$] but not for electrode sites in the third quartile [3rd: $t(7) = -0.08$, $P = 0.94$] (Fig. 3*C*). In DG, a significant relationship between speed and theta power was observed only for electrode sites in the septalmost quartile [1st: $t(7) = 5.71$, $P < 0.001$; 2nd: $t(6) = 1.04$, $P = 0.34$; Fig. 3*C*].

In summary, a positive relationship between speed and theta power was quite evident in all septal (1st quartile) electrode sites, with speed accounting for considerable variation in theta power at both CA1 (mean *r* value for CA1 sites in 1st quartile = 0.66 ± 0.07) and DG (mean *r* value for DG sites in 1st quartile = 0.31 ± 0.05) sites. Notably, locomotor speed accounted for more of the variability at CA1 sites than at DG sites within the first and second quartiles of the HPC (*P* values < 0.001; Fig. 3*C*). The more prominent relationship between speed and theta power in CA1, compared with DG sites, has been previously demonstrated by Montgomery and colleagues (2009; see Fig. 3). Their study noted clear differences across distinct laminar positions with greater variability across laminar subfields of CA1 (e.g., pyramidale vs. lacunosum moleculare). We also observed subtle differences across distinct laminar positions (see Supplemental Fig. S3). Regardless of laminar location within CA1, a prominent decrease in the speed-to-power relationship was observed across the septotemporal axis.

Theta power and locomotor speed within the EC. Theta LFPs were recorded at 13 electrode sites within the superficial layers of the EC in both the medial ($n = 7$) and lateral ($n = 6$) subdivisions of the EC (Fig. 1*F*). The power of theta signals from both MEA and LEA were moderately lower than those observed in the HPC, but no differences were observed between MEA and LEA sites (see Table 1).

Sites in both MEA and LEA showed significant speed modulation of theta power [MEA: $t(6) = 3.81$, $P < 0.01$; LEA: $t(5) = 15.10$, $P < 0.0001$], with no difference between MEA and LEA sites [$t(11) = 1.09$, $P = 0.30$; Fig. 3, *D* and *E*]. Locomotor speed predicted roughly 10–20% (mean $r^2 = 0.18$ for all EC sites) of variability at electrode sites in MEA and LEA. Thus the relationship of speed to theta power was less than that observed at septal HPC sites, suggesting that the relationship of speed to theta power within septal HPC sites is not necessarily a consequence of this phenomenon at EC sites. Certainly, our analysis was limited to 14 sites across the areal axis of the EC (see Fig. 1 as well as Supplemental Fig. S3). Given the topography of EC to HPC projections, one might expect locations in the most lateral band of the EC (subjacent the rhinal sulcus; Dolorfo and Amaral 1998a) to exhibit the largest speed-to-power relationship. Clearly, we did not observe any obvious differences among the more laterally located electrode sites, but most were located in the medial band of MEA and LEA, with only two sites approaching the region subjacent the rhinal sulcus. Further assessment of variation in the speed-to-power relationship across the areal surface of the EC is thus warranted.

Theta frequency and locomotor speed throughout the hippocampal formation. The relationship between theta frequency and locomotor speed was investigated in the same manner as the relationship between theta power and locomotor speed described above. Theta frequency was found to increase as a function of locomotor speed in all regions explored (Fig. 4). This positive relationship between locomotor speed and theta frequency can be seen for three simultaneously recorded sites across the septotemporal axis of CA1 in Fig. 4*A*. In opposition to the septotemporal gradient of the influence of locomotor speed on theta power, sites across the septotemporal axis of both CA1 and DG showed significant speed modulation of theta frequency. The relationship between locomotor speed and theta frequency did not vary across the septotemporal axis of either CA1 ($r = -0.35$, $P = 0.09$) or DG ($r = -0.18$, $P = 0.53$; Fig. 4*B*). Assessment of the speed modulation of theta frequency within individual quartiles of both CA1 and DG indicated that all regions of the hippocampus explored displayed significant speed modulation of theta frequency [CA1 1st: $t(4) = 18.73$, $P < 0.001$; 2nd: $t(11)$ 13.52, $P < 0.001$; 3rd: $t(7) = 12.32$, $P < 0.001$; DG 1st: $t(7) = 11.43$, $P < 0.001$; 2nd: $t(6) = 11.61$, $P < 0.001$; Fig. 4*C*]. In EC, theta frequency was speed modulated in both MEA and LEA [MEA: $t(6) = 3.25$, $P < 0.05$; LEA: $t(5) = 2.95$, $P < 0.05$; Fig. 4*D*]. Thus theta frequency was positively modulated by the locomotor speed of the animal in all regions of the hippocampal formation explored. Notably, the present results support relatively independent mechanisms for regulating hippocampal theta amplitude compared with theta frequency. A variety of evidence indicates a prominent role for the medial septal inputs in controlling theta amplitude, while a network including the nucleus reticularis pontis oralis (RPO) and hypothalamic nuclei (e.g., supramammillary nucleus) controls theta frequency (see Lee et al. 1994; Pan and McNaughton, 2004; Vertes and Kocsis 1997; Vertes et al. 2004 for reviews).

Rhinal-hippocampal and intrahippocampal theta coherence and locomotor speed. The relation between locomotor speed and theta coherence was examined between EC and DG sites (EC-DG pairs = 32) as well as CA1 (EC-CA1 pairs = 48). MEA and LEA sites were grouped together since there was no statistical difference between the two areas (*P* values > 0.50). Similar to changes in theta power, theta coherence between paired EC and HPC sites significantly increased as a function of locomotor speed when the pair included a septal HPC electrode site (Fig. 5*A*). Regression analysis of the septotemporal position (distance from septal pole) and the speed-related *r* value showed that theta coherence between EC-CA1 pairs and EC-DG pairs exhibited less relation to speed when HPC electrode sites were located at more temporal levels ($r = -0.44$, $P < 0.005$ for EC-CA1 pairs; $r = -0.55$, $P < 0.005$ for all EC-DG pairs regardless of areal position of the EC electrode; Fig. 5*B*). From examination of the data grouped by hippocampal quartiles, theta coherence increased in relation to locomotor speed only between EC-CA1 and EC-DG pairs within the septalmost quartile of the HPC [EC-CA1: $t(3) = 5.04$, $P = 0.02$; EC-DG: $t(12) = 6.30$, $P < 0.0001$; Fig. 5*C*]. Thus the speed-related increase in theta coherence between any EC electrode and any HPC electrode varied along the septotemporal axis. Importantly, the intrahippocampal coherence in relation to speed also exhibited variation along the septotemporal axis. Plotting the speed-related correlation coefficient among HPC electrode pairs by quartile, Fig. 5*D* illustrates that coherence among the septalmost elec-

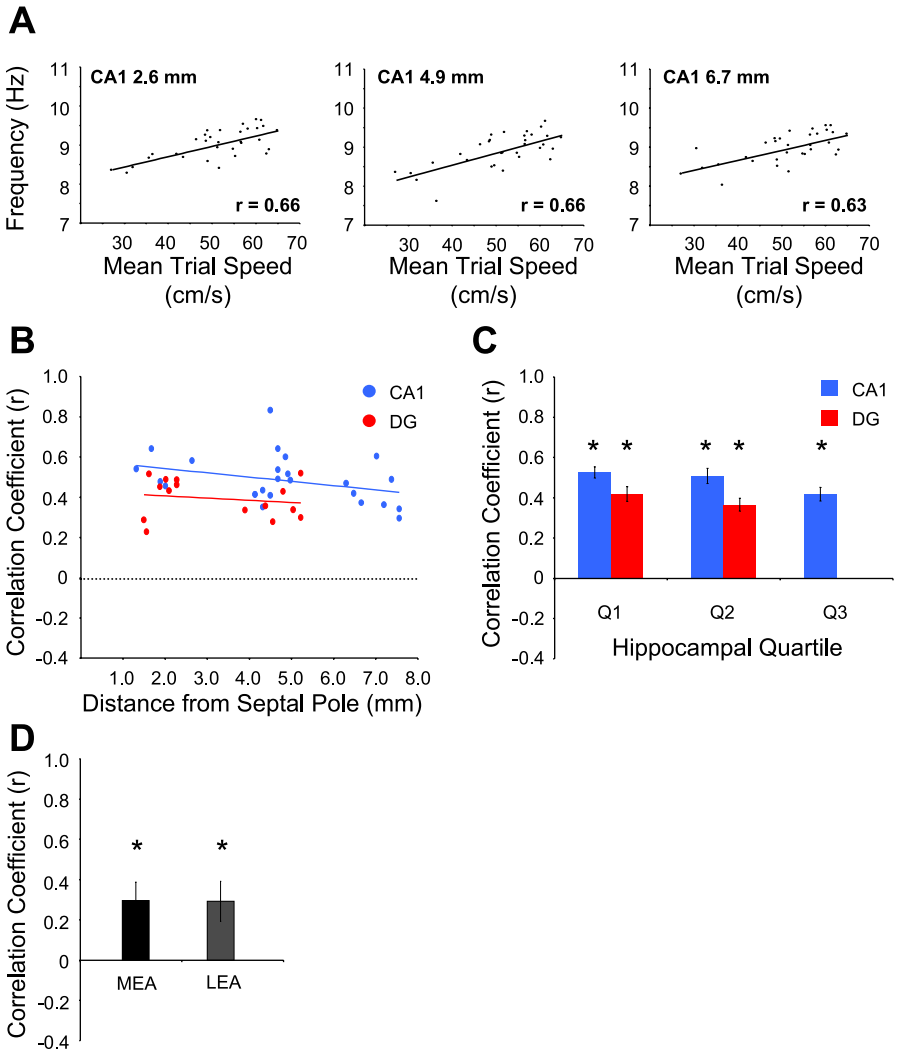

Fig. 4. Speed modulation of theta frequency throughout the hippocampal formation. *A*: the relationship between mean trial speed and theta frequency for 3 simultaneously recorded sites along the septotemporal axis of CA1 is shown during the baseline recording only. The distance of each recording site from the septal pole is displayed in each plot along with the correlation coefficient. Note that there is no change in the correlation coefficients with increasing distance from the septal pole. *B*: the positive relationship between locomotor speed and theta frequency is observed across the septotemporal axis of both CA1 and DG as indicated by the nonsignificant correlation between each electrode's distance from the septal pole and the speed vs. theta frequency correlation coefficients for each CA1 and DG electrode. *C*: all CA1 and DG electrodes were grouped according to septotemporal quartile in order to assess whether theta frequency was significantly speed modulated in each region. Theta frequency was significantly speed modulated in all quartiles investigated (*$P < 0.01$, *t*-test). *D*: theta frequency was also found to be speed modulated in both MEA and LEA (*$P < 0.01$, *t*-test).

trodes increased while coherence among more temporally located pairs decreased as a function of locomotor speed.

Theta power across repeated behavioral sessions. We collected data during an initial run session (baseline) of at least 50 trials and then returned rats to the linear track to run additional sessions of at least 50 trials at 5, 20, 60, and 120 min after the initial run session (Fig. 1*A*). In examining data across repeated recording sessions within a single day, it became obvious that there was a systematic decrease in theta power over sessions at more temporally located electrode sites. A clear downward shift in the linear best-fit line for the relationship between speed and theta power was observed at the more temporal aspects of both DG and CA1 without any significant change in the slope of the lines (Fig. 6*A*). This shift was not evident at septal HPC sites (Fig. 6*A*). To examine whether this decrease had any relation to running speed or time (habituation), we conducted a linear regression analysis factoring out speed across time points. The resulting standardized regression coefficients (β-values) reflect the change in theta power means from baseline to the postbaseline recordings controlling for the speed of the animal. The β-values were assessed with a within-electrode repeated-measures ANOVA. A significant time-dependent reduction in theta power was observed in the second and third quartiles of CA1, as well as within the second quartile of the DG [CA1-Q1 $F(3,12) = 3.49$, $P = 0.05$; CA1-Q2 $F(3,33) = 12.08$, $P < 0.001$; CA1-Q3 $F(3,21) = 6.99$, $P < 0.005$; DG-Q1 $F(3,21) = 1.76$, $P = 0.19$; DG-Q2 $F(3,18) = 7.58$, $P < 0.005$; Fig. 6*B*]. A significant decrease in theta power was observed among electrodes in the first quartile of the DG ($P < 0.01$; Fig. 6*B*), but this decrease did not vary across time points. No significant changes were observed among electrodes in the first quartile of CA1 (Fig. 6*B*). Thus the reduction in theta power observed at more temporally located recordings sites appears to represent habituation to sensory, motor, or motivational aspects of the behavior without any obvious relationship to differences in the overt motor act (e.g., speed of locomotion).

DISCUSSION

Dynamic variation in LFP signals (e.g., power and coherence) may serve as useful measures of change in the highly laminar and topographically organized afferent zones of hippocampal afferents. Such changes can be related to ongoing sensorimotor experience (e.g., speed), recent past behavioral experience (e.g., habituation over repeated testing), or cognitive processes (see, e.g., Kay 2005; Montgomery et al. 2009; Rizzuto et al. 2006; Shirvalkar et al. 2010; Tort et al. 2009; Ulanovsky and Moss 2007).

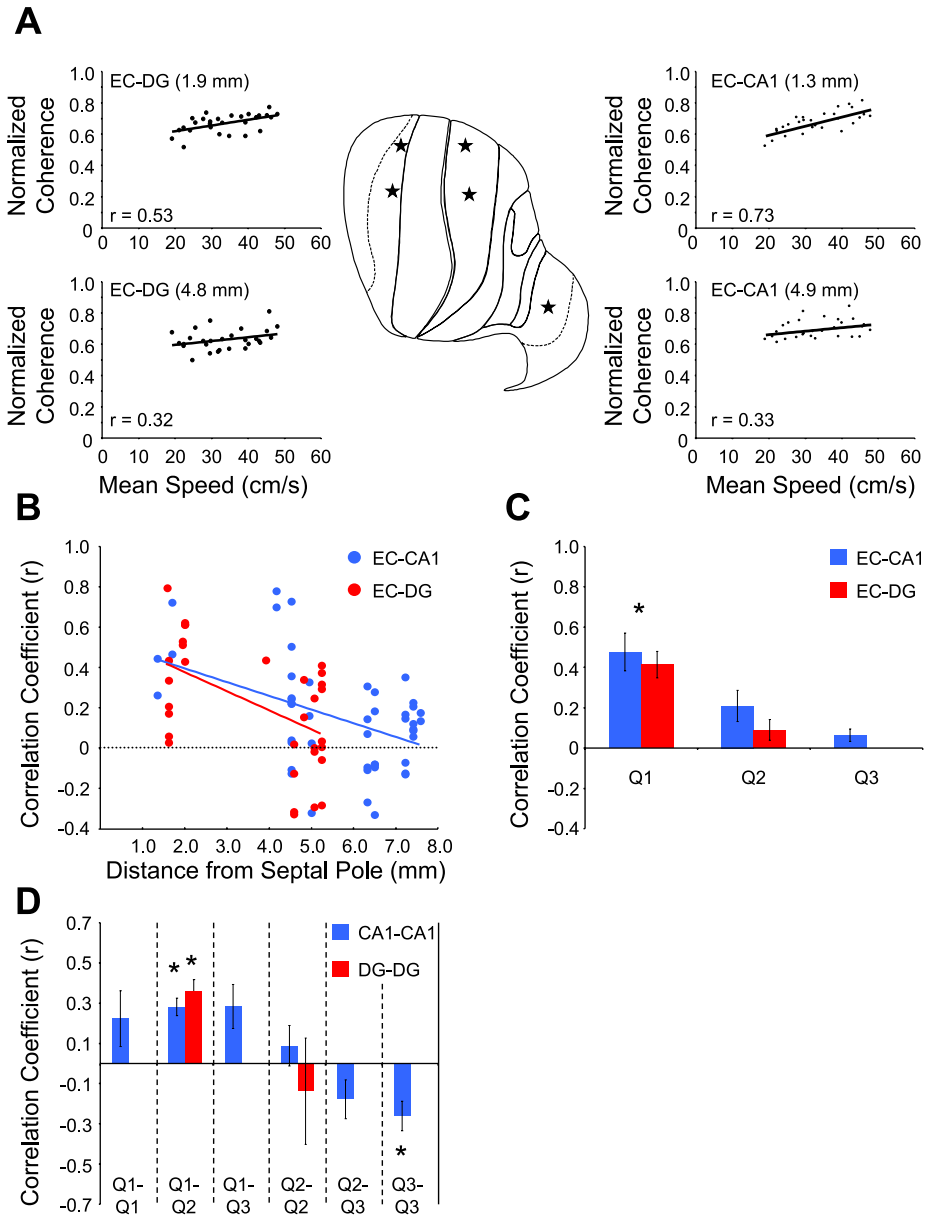

Fig. 5. Rhinal-hippocampal and intrahippocampal theta coherence and locomotor speed. *A*: flatmap (*middle*) shows 1 recording site in EC and 4 hippocampal sites. Scatterplots show the relationship between mean trial speed and theta coherence between the EC site and each of the 4 different hippocampal sites. Distance displayed in each plot is the distance of the hippocampal electrode site from the septal pole. Also displayed in each plot is the correlation coefficient for the relationship between speed and theta coherence for that electrode pair. Note that theta coherence between EC and the more temporal hippocampal electrodes is less speed modulated than theta coherence between EC and the septal hippocampal electrodes. *B*: the speed modulation of EC-CA1 and EC-DG theta coherence significantly decreases as a function of the distance from the septal pole of the hippocampal electrode. *C*: theta coherence between EC and the 1st quartile of CA1 and DG is speed modulated (*$P < 0.01$, *t*-test), while theta coherence between EC and all other quartiles is not speed modulated. *D*: theta coherence within the hippocampus is speed modulated when the electrodes are within the septal half, while theta coherence within more temporal aspects of CA1 actually decreases with increasing locomotor speed (*$P < 0.01$, *t*-test).

The present findings demonstrate substantial septotemporal variation in indices of theta LFPs as a function of sensorimotor experience and recent past behavioral experience. Foremost, we observed that theta power increased linearly as a function of speed at electrode sites in the septal HPC, accounting for 40–80% of the variability in theta power. The strength of this relationship diminished with distance from the septal pole. Second, the relationship between speed and theta power, and its decline across the long axis, were more prominent at CA1 sites compared with sites within the DG. Third, theta power increased with speed at all EC sites, including both LEA and MEA sites. The relationship between speed and theta power did not vary across the areal axis of the EC (LEA compared with MEA). Fourth, theta coherence between EC and HPC also exhibited a septotemporal gradient in its relationship to speed, such that coherence between EC and septal HPC sites was positively speed modulated, while coherence between EC and temporal HPC sites was not speed modulated. Fifth, theta coherence increased as a function of speed between pairs of septally located HPC electrodes, while theta coherence decreased between temporally located HPC pairs. Finally, we observed significant changes in theta power as a function of behavioral habituation (repeated runs on a linear maze). This habituation-related decrease in theta power was minimal at CA1 sites in the septal HPC and was most prominent at sites located distant from the septal pole.

Our most basic finding is that speed is a prominent predictor of theta indices (both power and coherence) in the septal HPC, accounting for 40–80% of the variability in theta power at septal CA1 sites. Speed, however, had a limited relation to variation in theta power at more temporal locations. The latter is consistent with previously observed differences in the speed-to-power relationship across the longitudinal axis observed by Maurer and colleagues (2005) with regard to both amplitude of theta field potential and the change in place field firing rate as a function of locomotor speed (see Fig. 4, Table 6 in Maurer et al. 2005). Differences in the speed-to-power relationship in the present study were not directly attributable to a decrease in the

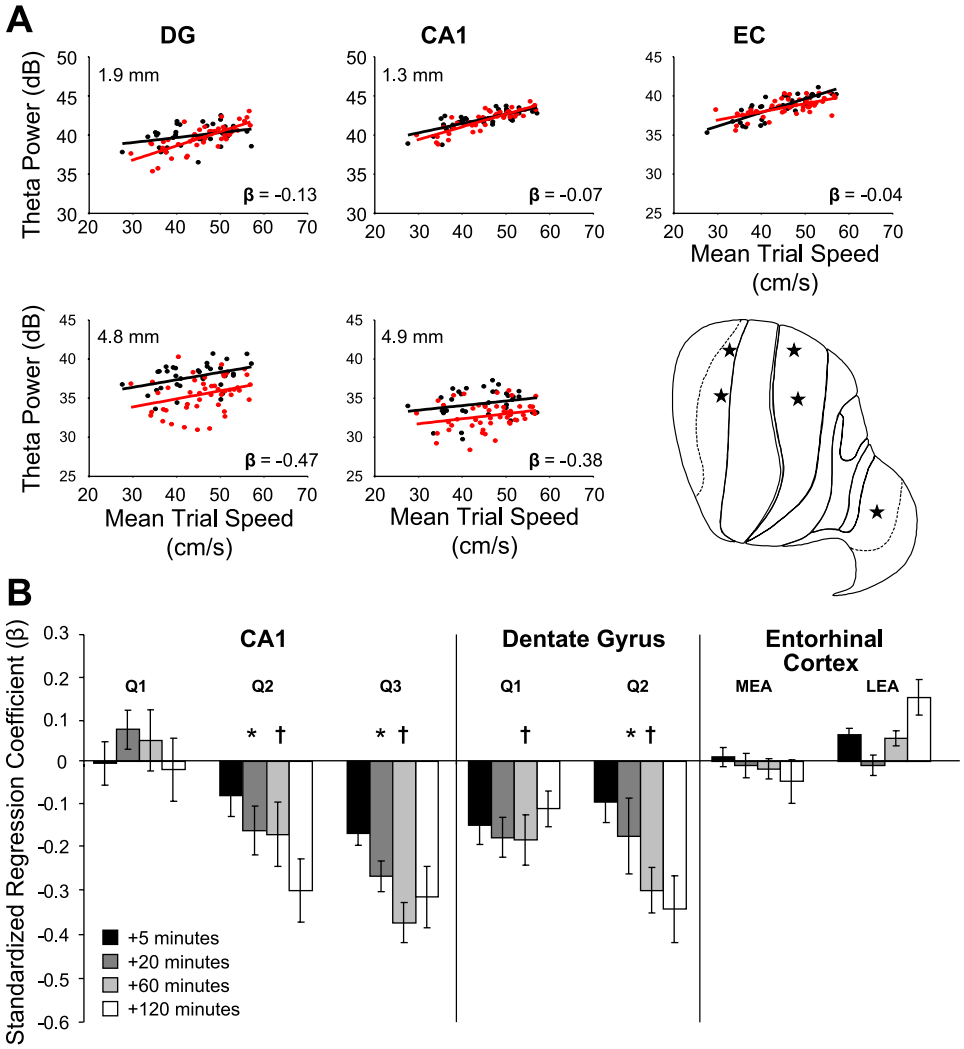

Fig. 6. Theta power habituates at temporal levels. *A*: flatmap displays 5 simultaneous recording sites (same as in Fig. 2). Scatterplots show theta power as a function of mean trial speed during the baseline recording (black) and the 5th recording session of the day that was initiated 120 min after the cessation of the baseline recording (red). The distance from the septal pole is indicated for the hippocampal sites, as well as the standardized regression coefficients (β) for each site. A clear downward shift in the linear best fit line can be seen in the more temporal DG and CA1 sites, demonstrating a within-day habituation of theta power. *B*: mean β-values for all regions investigated. There was a significant effect of time in the 2nd and 3rd quartiles of CA1 and the 2nd quartile of DG, while the 1st quartile of DG showed a decrease in theta power without an effect of time. *Significant time-dependent reduction in theta power for an individual quartile as assessed by repeated-measures ANOVA (P values < 0.01). †Significant decrease in theta power from baseline for an individual quartile (P values < 0.01).

variability of the theta signal but likely reflect a fundamental difference in the mechanisms/circuitry that govern theta across the long axis. We observed significant changes in theta power associated with repeated behavioral testing within a daily session that also exhibited regional (septotemporal) variation. These data suggest that the theta LFP signal is highly dynamic, reflecting clear variation in the septotemporal synchronization of synaptic input across the dendritic field of hippocampal neurons. Such variation can be compared in many ways to alterations in the BOLD signal of human functional MRI (fMRI) studies, where changes across the anterior-posterior axis of the HPC have been observed in relation to novelty, familiarity, and habituation (Stern et al. 1996; Strange et al. 1999; see Kumaran and Maguire 2009 for review).

Anatomic differences across the septotemporal axis. Areal variation in theta signals may reflect variation in the topography of several afferent inputs that synapse on the dendritic field of CA1 and DG neurons. There are three major populations of excitatory glutamatergic afferents that are critical to theta current generation. First, projections from layer 2 EC neurons target the distal dendrites of dentate granule neurons (as well as local GABAergic neurons). Second, projections from layer 3 EC neurons target the distal dendrites of CA1 neurons. These EC projections originate from segregate areal bands that project in a topographic manner along the septotemporal axis (Dolorfo and Amaral 1998a, 1998b). Thus the EC projections provide a potential source of variation in the theta signal across the long axis. Third, intrinsic hippocampal associational projections (CA3 to CA1 and mossy cells to DG) project extensively across the long axis (Amaral and Witter 1995; Ishizuka et al. 1990), providing a potential mechanism for synchronizing neural activity.

While the topography of EC afferents could contribute to the observed differences in theta coherence, we found no variation in the relationship between speed and any theta index across the areal surface of the EC. While our mapping of the EC was limited, we have no evidence to support areal variation in the speed-to-power relationship at EC sites. Deshmukh and colleagues (2010) have illustrated clear differences in theta power and the theta modulation of EC neurons between the MEA and LEA. Our study was limited to 14 sites across the areal surface of the EC, and few of the sites (see Fig. 1*F*) extended to the lateral band of the EC. Neurons in the most lateral band of the EC in both the MEA and LEA, subjacent the rhinal sulcus and at the dorsocaudal extreme of the EC, innervate the septal 50% of the HPC (see Dolorfo and Amaral 1998a, 1998b). Thus additional mapping of variations in the theta signal and its relation to speed will be required to determine the influence of

EC inputs on variation in the speed-to-theta power relationship across the septotemporal axis of the HPC.

In addition to the excitatory EC inputs, any number of studies point to the prominent role of subcortical afferents including glutamatergic afferents (e.g., supramammillary nucleus), GABAergic afferents (most prominently from the medial septum), and several neuromodulatory inputs in generating and influencing the theta signal via direct afferent input to the HPC and/or indirectly via medial septal afferents (see Bland 1986; Bland and Oddie 2001; Lee et al. 1994; Vertes and Kocsis 1997; Vertes et al. 2004).

While many studies have demonstrated variation in the discharge rate of subcortical neurons across theta states (e.g., theta vs. nontheta), few studies have systematically examined changes in neuronal firing rate as a function of locomotor speed. King and colleagues (1998) described that many (65%), but not all, medial septal neurons exhibit a linear increase in burst discharge rate as a function of speed. Thus medial septal inputs may provide a key source of variation in relaying speed information across the septotemporal axis. Such speed information may be transmitted to septal neurons via supramammillary, midline thalamic, or other brain stem afferents. Importantly, there is considerable topographic variation in the organization of ascending subcortical afferents both in their direct projections to the HPC as well as in their indirect inputs to medial septal neurons, which also project topographically throughout the septotemporal axis (Amaral and Kurz 1985; Amaral and Witter 1995).

Furthermore, our analyses indicated that while there were differences in the relationship between speed and theta power across the septotemporal axis, we did not observe any differences in the relationship of speed to theta frequency. While theta frequency increases in relation to locomotor speed, there was no variability in this relationship across the septotemporal axis of the HPC or across distinct sites within the EC. The fundamental difference between the variations in speed to power compared with speed to frequency across the septotemporal axis supports the idea that distinct subcortical circuits regulate theta power and frequency. A variety of evidence indicates that a network including the RPO and hypothalamic nuclei (e.g., supramammillary nucleus) contribute to theta frequency independent of theta power (see Pan and McNaughton 2004; Vertes and Kocsis 1997; Vertes et al. 2004 for reviews).

Functional differentiation across the septotemporal axis. Historically, significant emphasis has been placed on examining the functionality of distinct hippocampal subregions within the trisynaptic circuit (DG > CA3 > CA1) rather than functional differences across the areal or longitudinal expanse of the HPC, which in the rodent is referred to as the septotemporal axis. The rodent septal pole is most similar to the posterior HPC in humans, while the temporal pole is similar to the anterior aspect of the HPC. The septotemporal axis of the HPC is analogous to an areal region of the neocortex and receives topographically organized input from distinct areal regions of the EC. Thus the septal 50% of the HPC receives input from lateral band EC neurons subjacent to the rhinal sulcus (Dolorfo and Amaral 1998a, 1998b). The topographic organization of EC inputs may convey relatively segregate domains of associative sensory input to different septotemporal levels of the HPC (Burwell and Amaral 1998; Lavenex and Amaral 2000). A variety of behavioral studies based largely on lesion data in rodents and neuroimaging data in humans support functional differentiation of hippocampal circuits along the long axis (Moser et al. 1995; Strange et al. 1999; see Bannerman et al. 2004 for review). Additionally, there is considerable septotemporal variation in neuronal markers (see, e.g., Gusev et al. 2005), neuromodulation of plasticity (Maggio and Segal 2007), and differences in the experiences that influence neurogenesis along the long axis (Snyder et al. 2009).

Our laboratory is particularly interested in synchronicity in theta along the septotemporal axis of the HPC and its relation to the EC input, with the general hypothesis that under distinct sensory or behavioral conditions theta coherence will increase among functional interactive domains, or decrease between less interactive domains. While theta is clearly coherent across the long axis, we have reported that there is a general decrease in theta coherence across the long axis during REM sleep (Sabolek et al. 2009; see also Royer et al. 2010). The present findings demonstrate a general increase in power and coherence in relation to locomotor speed across the most septal aspect of the HPC that is sustained over repeated behavioral experience (see Fig. 6). In contrast, there is a minimal alteration in theta power in relation to locomotor speed in the more temporal aspects of the HPC and a systematic decrease over repeated behavioral experience (see Fig. 6). Typically, rats are trained and tested as in this case in the same environmental context, so the observed changes occur in an environment that is highly familiar to the animal. Recent findings in our laboratory demonstrate that novel spatial environments (while the rat is performing the exact same behavior, running along a linear path) increase theta power and theta coherence across much of the septotemporal axis (S. C. Penley and J. J. Chrobak, unpublished observations). Thus it appears that changes in theta power and coherence are sensitive to both novelty and habituation. As observed in the human neuroimaging studies, the LFP signal variation in rodents also demonstrates considerable variability across the septotemporal axis.

Summary. Theta LFP signals within the hippocampal formation reflect the dynamic interaction of competing and cooperating inputs, which vary across the dendritic field of HPC and EC neurons. In this regard, systematic assessment of this signal at various laminar and septotemporal positions can provide a spatial and temporal window into the dynamic flow of afferent input. Systematic changes in theta potentials have been linked to changes in sensorimotor integration, the flow of sensory input, as well as cognitive/memory functions. The present findings demonstrate a dynamic and distributed pattern of theta LFPs across the septotemporal axis of the HPC in relation to locomotor speed and recent past experience.

GRANTS

This work was supported by National Science Foundation 0090451 to J. J. Chrobak and M. A. Escabí.

DISCLOSURES

No conflicts of interest, financial or otherwise, are declared by the author(s).

REFERENCES

Amaral DG, Kurz J. An analysis of the origins of the cholinergic and noncholinergic septal projections to the hippocampal formation of the rat. *J Comp Neurol* 240: 37–59, 1985.

Amaral DG, Witter MP. The three-dimensional organization of the hippocampal formation: a review of anatomical data. *Neuroscience* 31: 371–391, 1995.

Bannerman DM, Rawlins JN, McHugh SB, Deacon RM, Yee BK, Bast T, Zhang WN, Pothuizen HH, Feldon J. Regional dissociations within the hippocampus—memory and anxiety. *Neurosci Biobehav Rev* 28: 273–283, 2004.

Bland BH. Physiology and pharmacology of hippocampal formation theta rhythms. *Prog Neurobiol* 26: 1–54, 1986.

Bland BH, Oddie SD. Theta band oscillation and synchrony in the hippocampal formation and associated structures: the case for its role in sensorimotor integration. *Behav Brain Res* 127: 119–136, 2001.

Bouwman BM, van Lier H, Nitert HE, Drinkenburg WH, Coenen AM, van Rijn CM. The relationship between hippocampal EEG theta activity and locomotor behaviour in freely moving rats: effects of vigabatrin. *Brain Res Bull* 64: 505–509, 2005.

Bragin A, Jando G, Nadasdy Z, Hetke J, Wise K, Buzsaki G. Gamma (40–100 Hz) oscillation in the hippocampus of the behaving rat. *J Neurosci* 15: 47–60, 1995.

Brankack AJ, Stewart M, Fox SE. Current source density analysis of the hippocampal theta rhythm: associated sustained potentials and candidate synaptic generators. *Brain Res* 615: 310–327, 1993.

Bullock TH, Buzsaki G, McClune MC. Coherence of compound field potentials reveals discontinuities in the CA1-subiculum of the hippocampus of the freely-moving rat. *Neuroscience* 38: 609–619, 1990.

Burwell RD, Amaral DG. Perirhinal and postrhinal cortices of the rat: interconnectivity and connections with the entorhinal cortex. *J Comp Neurol* 391: 293–321, 1998.

Buzsaki G. Theta oscillations in the hippocampus. *Neuron* 33: 325–340, 2002.

Deshmukh SS, Yoganarasimha D, Voicu H, Knierim JJ. Theta modulation in the medial and lateral entorhinal cortices. *J Neurophysiol* 104: 994–1006, 2010.

Dolorfo CL, Amaral DG. Entorhinal cortex of the rat: topographic organization of the cells of origin of the perforant path projections to the dentate gyrus. *J Comp Neurol* 398: 25–48, 1998a.

Dolorfo CL, Amaral DG. Entorhinal cortex of the rat: organization of intrinsic connections. *J Comp Neurol* 398: 49–82, 1998b.

Efron B, Tibshirani RJ. *An Introduction to the Bootstrap*. New York: Chapman & Hall, 1993.

Feder R, Ranck JB Jr. Studies on single neurons in dorsal hippocampal formation and septum in unrestrained rats. II. Hippocampal slow waves and theta cell firing during bar pressing and other behaviors. *Exp Neurol* 41: 532–555, 1973.

Gage FH, Thompson RG. Differential distribution of norepinephrine and serotonin along the dorsal-ventral axis of the hippocampal formation. *Brain Res Bull* 5: 771–773, 1980.

Green JD, Arduini AA. Hippocampal electrical activity in arousal. *J Neurophysiol* 17: 533–557, 1954.

Gusev PA, Cui C, Alkon DL, Gubin AN. Topography of Arc/Arg3.1 mRNA expression in the dorsal and ventral hippocampus induced by recent and remote spatial memory recall: dissociation of CA3 and CA1 activation. *J Neurosci* 25: 9384–9397, 2005.

Ishizuka N, Weber J, Amaral DG. Organization of intrahippocampal projections from CA3 pyramidal cells in the rat. *J Comp Neurol* 295: 580–623, 1990.

Jeewajee A, Barry C, O'Keefe J, Burgess N. Grid cells and theta as oscillatory interference: electrophysiological data from freely moving rats. *Hippocampus* 18: 1175–1185, 2008.

Jutras MJ, Buffalo EA. Synchronous neural activity and memory formation. *Curr Opin Neurobiol* 20: 150–155, 2010.

Kay LM. Theta oscillations and sensorimotor performance. *Proc Natl Acad Sci USA* 102: 3863–3868, 2005.

King C, Recce M, O'Keefe J. The rhythmicity of cells of the medial septum/diagonal band of Broca in the awake freely moving rat: relationships with behaviour and hippocampal theta. *Eur J Neurosci* 10: 464–477, 1998.

Kumaran D, Maguire EA. Novelty signals: a window into hippocampal information processing. *Trends Cogn Sci* 13: 47–54, 2009.

Lavenex P, Amaral DG. Hippocampal-neocortical interaction: a hierarchy of associativity. *Hippocampus* 10: 420–430, 2000.

Lee MG, Chrobak JJ, Sik A, Wiley RG, Buzsáki G. Hippocampal theta activity following selective lesion of the septal cholinergic system. *Neuroscience* 62: 1033–1047, 1994.

Leung LWS. Spectral analysis of hippocampal EEG in the freely moving rat: effects of centrally active drugs and relations to evoked potentials. *Electroencephalogr Clin Neurophysiol* 60: 65–77, 1985.

Lorch RF Jr, Myers JL. Regression analyses of repeated measures data in cognitive research. *J Exp Psychol Learn Mem Cogn* 16: 149–157, 1990.

Maggio N, Segal M. Striking variations in corticosteroid modulation of long-term potentiation along the septotemporal axis of the hippocampus. *J Neurosci* 27: 5757–5765, 2007.

Maurer AP, VanRhoads SR, Sutherland GR, Lipa P, McNaughton BL. Self-motion and the origin of differential spatial scaling along the septotemporal axis of the hippocampus. *Hippocampus* 15: 841–852, 2005.

McFarland WL, Teitelbaum H, Hedges EK. Relationship between hippocampal theta activity and running speed in the rat. *J Comp Physiol Psychol* 88: 324–328, 1975.

Montgomery S, Betancur MI, Buzsaki G. Behavior-dependent coordination of multiple theta dipoles in the hippocampus. *J Neurosci* 29: 1381–1394, 2009.

Moser MB, Moser EI, Forrest E, Andersen P, Morris RG. Spatial learning with a minislab in the dorsal hippocampus. *Proc Natl Acad Sci USA* 92: 9697–9701, 1995.

Nyhus E, Curran T. Functional role of gamma and theta oscillations in episodic memory. *Neurosci Biobehav Rev* 34: 1023–1035, 2010.

Pan WX, McNaughton N. The supramammillary area: its organization, functions and relationship to the hippocampus. *Prog Neurobiol* 74: 127–166, 2004.

Petsche H, Stumpf C, Gogolak G. The significance of the rabbit's septum as a relay station between the midbrain and the hippocampus. I. The control of hippocampus arousal activity by the septum cells. *Electroencephalogr Clin Neurophysiol* 14: 202–211, 1962.

Pitkanen A, Pikkarainen M, Nurminen N, Ylinen A. Reciprocal connections between the amygdala and the hippocampal formation, perirhinal cortex and postrhinal cortex in rat. A review. *Ann NY Acad Sci* 911: 369–391, 2000.

Rizzuto DS, Madsen JR, Bromfield EB, Schulze-Bonhage A, Kahana MJ. Human neocortical oscillations theta phase differences between encoding and retrieval. *Neuroimage* 31: 1352–1358, 2006.

Rivas J, Gaztelu JM, García-Austt E. Changes in hippocampal cell discharge patterns and theta rhythm spectral properties as a function of walking velocity in the guinea pig. *Exp Brain Res* 108: 113–118, 1996.

Roark RM, Escabi MA. B-spline design of maximally flat and prolate spheroidal-type FIR filters. *IEEE Trans Signal Processing* 47: 701–716, 1999.

Royer S, Sirota A, Patel J, Buzsaki G. Distinct representations and theta dynamics in dorsal and ventral hippocampus. *J Neurosci* 30: 1777–1787, 2010.

Sabolek HR, Penley SC, Hinman JR, Bunce JG, Markus EJ, Escabi M, Chrobak JJ. Theta and gamma coherence along the septotemporal axis of the hippocampus. *J Neurophysiol* 101: 1192–1200, 2009.

Shirvalkar PR, Rapp PR, Shapiro ML. Bidirectional changes to hippocampal theta-gamma comodulation predict memory for recent spatial episodes. *Proc Natl Acad Sci USA* 107: 7054–7059, 2010.

Sinnamon HM. Decline in hippocampal theta activity during cessation of locomotor approach sequences: amplitude leads frequency and relates to instrumental behavior. *Neuroscience* 140: 779–790, 2006.

Snyder JS, Radik R, Wojtowicz JM, Cameron HA. Anatomical gradients of adult neurogenesis and activity: young neurons in the ventral dentate gyrus are activated by water maze training. *Hippocampus* 19: 360–370, 2009.

Stern CE, Corkin S, González RG, Guimaraes AR, Baker JR, Jennings PJ, Carr CA, Sugiura RM, Vedantham V, Rosen BR. The hippocampal formation participates in novel picture encoding: evidence from functional magnetic resonance imaging. *Proc Natl Acad Sci USA* 93: 8660–8665, 1996.

Strange BA, Fletcher PC, Henson RN, Friston KJ, Dolan RJ. Segregating the functions of human hippocampus. *Proc Natl Acad Sci USA* 96: 4034–4039, 1999.

Swanson LW, Wyss JM, Cowan WM. An autoradiographic study of the organization of intrahippocampal association pathways in the rat. *J Comp Neurol* 181: 681–715, 1978.

Teitelbaum H, McFarland WL. Power spectral shifts in hippocampal EEG associated with conditioned locomotion in the rat. *Physiol Behav* 7: 545–549, 1971.

Thompson CL, Pathak SD, Jeromin A, Ng LL, MacPherson CR, Mortrud MT, Cusick A, Riley ZL, Sunkin SM, Bernard A, Puchalski RB, Gage

FH, Jones AR, Bajic VB, Hawrylycz MJ, Lein ES. Genomic anatomy of the hippocampus. *Neuron* 60: 1010–1021, 2008.

Tort AB, Komorowski RW, Manns JR, Kopell NJ, Eichenbaum H. Theta-gamma coupling increases during the learning of item-context associations. *Proc Natl Acad Sci USA* 106: 20942–20947, 2009.

Ulanovsky N, Moss CF. Hippocampal cellular and network activity in freely moving echolocating bats. *Nat Neurosci* 10: 224–233, 2007.

Vertes RP, Kocsis B. Brainstem-diencephalo-septohippocampal systems controlling the theta rhythm of the hippocampus. *Neuroscience* 81: 893–926, 1997.

Vertes RP, Hoover WB, Viana Di Prisco G. Theta rhythm of the hippocampus: subcortical control and functional significance. *Behav Cogn Neurosci Rev* 3: 173–200, 2004.

Welch PD. The use of fast Fourier transform for the estimation of power spectra: a method based on time averaging over short, modified periodograms. *IEEE Trans Audio Electroacoust* 15: 70–73, 1967.

Whishaw IQ, Vanderwolf CH. Hippocampal EEG and behavior: changes in amplitude and frequency of RSA (theta rhythm) associated with spontaneous and learned movement patterns in rats and cats. *Behav Biol* 8: 461–484, 1973.

Witter MP. The perforant path: projections from the entorhinal cortex to the dentate gyrus. *Prog Brain Res* 163: 43–61, 2007.

Wyble BP, Hyman JM, Rossi CA, Hasselmo ME. Analysis of theta power in hippocampal EEG during bar pressing and running behavior in rats during distinct behavioral contexts. *Hippocampus* 14: 662–674, 2004.

Vanderwolf CH. Hippocampal electrical activity and voluntary movement in the rat. *Electroencephalogr Clin Neurophysiol* 26: 407–418, 1969.